Journal of Pathology
J Pathol 2011; **225:** 232–242
Published online 27 June 2011 in Wiley Online Library
(wileyonlinelibrary.com) DOI: 10.1002/path.2931

ORIGINAL PAPER

Deregulated miR-155 promotes Fas-mediated apoptosis in human intervertebral disc degeneration by targeting FADD and caspase-3

Hai-Qiang Wang,[1†] Xiao-Dong Yu,[1†] Zhi-Heng Liu,[1†] Xin Cheng,[2] Dino Samartzis,[3] Lin-Tao Jia,[2] Sheng-Xi Wu,[4] Jing Huang,[4] Jing Chen[4] and Zhuo-Jing Luo[1*]

[1] *Institute of Orthopaedics, Xijing Hospital, Fourth Military Medical University, Xi'an, People's Republic of China*
[2] *Department of Biochemistry and Molecular Biology, Fourth Military Medical University, Xi'an, People's Republic of China*
[3] *Department of Orthopaedics and Traumatology, University of Hong Kong, Pokfulam, Hong Kong, SAR China*
[4] *Department of Anatomy and K. K. Leung Brain Research Centre, Fourth Military Medical University, Xi'an, People's Republic of China*

**Correspondence to: Zhuo-Jing Luo, Institute of Orthopaedics, Xijing Hospital, 15 Changle Western Road, Fourth Military Medical University, Xi'an 710032, People's Republic of China. e-mail: zjluo@fmmu.edu.cn*

†These authors contributed equally to this study.

Abstract

The role of apoptosis in the pathogenesis of intervertebral disc degeneration (IDD) remains enigmatic. Accumulating evidence has shown that the apoptotic machinery is regulated by miRNAs. We hypothesized that miRNAs might contribute to apoptosis in IDD. We have found that 29 miRNAs were differentially expressed and miR-155 was down-regulated in degenerative nucleus pulposus (NP). The deregulation of miR-155 was further verified using real-time PCR (0.56 fold, $p < 0.05$). Bioinformatics target prediction identified FADD and caspase-3 as putative targets of miR-155. Furthermore, miR-155 inhibited FADD and caspase-3 expression by directly targeting their 3′-UTRs, which was abolished by mutation of the miR-155 binding sites. *In vitro* up-regulation of miR-155 in human NP cells by transfection with lentiviral pre-miR-155 resulted in repression of FADD and caspase-3; whereas knockdown of miR-155 with lentiviral antigomiR-155 led to over-expression of FADD and caspase-3. Also, Fas-mediated apoptosis was increased when antagonizing miR-155 and decreased when using pre-miR-155 in human NP cells. In addition, we presented direct evidence of NP cells undergoing apoptosis in IDD tissues using transmission electron microscopy analysis. Moreover, a combination of *in situ* hybridization (ISH) and immunohistochemistry (IHC) revealed that miR-155 expressed in the cytoplasm of human NP cells with reverse correlation with FADD and caspase-3. In summary, this is the first study addressing the underlying mechanisms of IDD in terms of apoptosis and miRNAs. Furthermore, caspase-3 is identified as a novel target of miR-155. Our results suggest that deregulated miR-155 promotes Fas-mediated apoptosis in human IDD by targeting FADD and caspase-3, implicating an aetiological and therapeutic role of miR-155 in IDD.

Keywords: disc degeneration; nucleus pulposus; miRNAs; miR-155; apoptosis; FADD; caspase-3

Received 28 December 2010; Revised 2 March 2011; Accepted 3 April 2011

No conflicts of interest were declared.

Introduction

Intervertebral disc degeneration (IDD) is associated with low back pain as a global burden with severe health-care and socioeconomic consequences [1,2]. The aetiology of IDD has been ascribed to various factors, ie polymorphisms in various genes [3,4], an increase in apoptosis and necrosis [5,6], hyperphysiological loading or overload [7,8] and aberrant MMPs and inflammatory cytokines [9–11]. However, the underlying mechanisms of IDD remain largely unknown with particular reference to the increase in apoptosis. Recently, there has been accumulating evidence addressing the immune privilege pertaining to the molecular mechanisms of IDD. The immune privilege of tissues is not only owing to the avascular hallmark but to a molecular mechanism, the local expression of FasL [12,13].

The intervertebral disc is composed of an outer fibrous layer, the annulus fibrosus, and an inner gelatinous core rich in proteoglycans, the nucleus pulposus (NP). The adult human NP consists mainly of small chondrocyte-like cells other than the alleged notochondral cells [14,15]. It has been noted that FasL exists in human intervertebral disc cells, the chief of which are NP cells [16,17].

The expression of FasL by NP cells could induce apoptosis of invading Fas-positive activated cytotoxic T-lymphocytes (CTLs), contributing to the immune privilege of NP. The FasL–Fas signalling pathway primarily pertains to several key proteins and caspases,

the chief of which are Fas-associated death domain-containing protein (FADD) and caspase-3 [18,19]. This death receptor pathway represents the extrinsic apoptotic signalling pathway, whereas the intrinsic pathway originates from the mitochondria and involves the activation of the Bcl-2 family [5,20]. However, Fas–FasL–FADD signalling was also found to participate in the intrinsic pathway. It has been noted that both the extrinsic and intrinsic pathways play essential roles in the apoptosis of human NP cells [5].

Accumulating evidence has shown that the apoptotic machinery is regulated by the newly defined small non-coding RNAs, miRNAs [21]. miRNAs control gene expression by targeting mRNAs and triggering either translation repression or RNA degradation [22,23]. A single miRNA is capable of regulating the expression of many target genes, whereas a target gene can also be regulated by several miRNAs [22,24]. The hundreds of miRNAs that have been identified regulate up to approximately 30% of all protein-encoding genes in human [22]. In animals, single-stranded miRNA binds the 3′-untranslated region (3′-UTR) of its target mRNA, termed miRNA response elements, causing the degradation or translational repression of the mRNA. These miRNAs act as key regulators in a wide variety of biological processes, including proliferation, differentiation, apoptosis, organ development and inflammatory diseases [25,26].

miR-155 is amongst the well-documented miRNAs involved in the regulation of immunological responses and apoptotic pathways [27]. As a multi-functional miRNA, miR-155 is expressed in diverse tissues [26]. Moreover, the aberrant expression of miR-155 is found to be associated with various diseases [28,29]. Given that miR-155 is crucially involved in apoptotic pathways, as well as disorders characterized by abnormal immune response and apoptosis, we assumed that miR-155 might play a role in the process of IDD. To date, no studies have addressed the aetiology of IDD from the point of miRNAs. Accordingly, the aim of this study was to address the role of miR-155 in IDD and to further clarify the underlying mechanisms of IDD.

Materials and methods

Sample collection

The study was approved by the institutional ethics review board (No. 20090611-3) with written informed consents obtained from each patient. Human NP specimens were collected from patients with idiopathic scoliosis and IDD as control [$n = 12$; average age 21.7 (range 18–38) years] and degenerative [$n = 12$; average age 30.2 (range 26–39) years] NP samples. Disc specimens were classified as grade II (idiopathic scoliosis discs) and grade IV (IDD discs) according to MRI [30]. The NP tissues were dissected carefully under magnification and subsequently managed under various schemes according to the corresponding procedures.

RNA isolation

Total RNA from cryostat tissues or isolated cells was isolated by TRIzol (Invitrogen, Carlsbad, CA, USA) and RNeasy mini kit (Qiagen, Valencia, CA, USA) according to the manufacturer's instructions. RNA integrity was monitored by electrophoresis in 8% denaturing polyacrylamide gels.

miRNAs microarray

The isolated NP tissues were snap-frozen in liquid nitrogen and subsequently stored at −70 °C. The frozen tissues or freshly isolated NP cells were homogenized and total RNA was extracted. RNA quality control was achieved by RNA electrophoresis. RNA labelling and hybridization on miRNA microarray chips were performed as previously described [31] (see Supporting information, Table S2). The results were visualized with Tree View.

Real-time PCR

qRT–PCR for miR-155 in NP cells was performed using TaqMan miRNA assays. In brief, miRNAs were reverse-transcribed to cDNAs, using a High-Capacity cDNA Archive Kit (ABI, Foster City, CA, USA). miR-155-specific stem–loop RT primers were used according to the manufacturer's instructions (TaqMan MicroRNA Assays Kit, ABI; see Supporting information, Table S1). RNA concentrations were determined using a NanoDrop instrument (NanoDrop, Wilmington, DE, USA).The levels of miR-155 were normalized to U6 controls. All RT reactions, including U6 controls, were run in triplicate in a GeneAmp PCR 9700 Thermocycler (ABI). The relative amounts of miR-155 were calculated using the comparative Ct ($2^{-\Delta\Delta Ct}$) method [32].

Detection of miRNA by *in situ* hybridization (ISH) and its attendant target by immunohistochemistry (IHC) in frozen sections

Tissues were fixed in 4% paraformaldehyde/phosphate-buffered saline (PBS), post-fixed with the same fixative and cut into 20 μm sections on a freezing microtome.

Detection of miR-155 and its putative targets by locked nucleic acid ISH and IHC

To detect and localize miR-155, we exploited the higher specificity and hybridization efficiency of locked nucleic acid (LNA) probes in frozen human NP tissues [33,34]. LNA hybridization probes labelled with digoxigenin (DIG) complementary to human mature miR-155 and negative controls (scramble probes) were purchased from Exiqon (Copenhagen, Denmark). The miR-155 sequences are given at: http://www.microrna.org. *In situ* hybridization (ISH) reactions were carried out as described previously [33–35]. Briefly, slides were subjected to proteinase K digestion for 10 min and subsequently prehybridization

buffer for 4 h. LNA probe (2 pM/μl) was denatured at 80 °C for 5 min and then hybridized for 7–15 h at 53 °C. The slides were then washed in 0.1 × SSC for 5 min at 53 °C and then incubated in anti-DIG Fab fragments in blocking buffer (1 : 2000 dilution) for 1 h at room temperature, and then in NBT/BCIP chromogen at 37 °C with monitoring under the microscope.

Subsequently, the sections were stained with antibodies followed by biotinylated secondary antibodies, as previously described [36]. Primary antibodies were against FADD (Abcam, Cambridge, MA, USA) and caspase-3 (Abcam), followed by biotinylated goat anti-rabbit IgG antibody (Vector Laboratories, Burlingame, CA, USA).

Immunohistochemistry

Frozen sections of samples of human NP were stained with antibodies followed by secondary antibodies. The aforementioned primary and secondary antibodies were used to detect the distribution of FADD and caspase-3. Frozen sections of human NP were stained with antibodies, followed by fluorescence-conjugated secondary antibodies. The aforementioned primary antibodies were used, followed by Alexa 488-conjugated goat anti-rabbit secondary antibodies (Molecular Probes, Eugene, OR, USA). 4′, 6-Diamidino-2-phenylindole (DAPI) staining was used as the final step in the fluorescent staining procedure to label the cell nuclei.

pFL-FADD 3′-UTR and pFL-caspase-3 3′-UTR vector construction and luciferase reporter assay

The 3′-UTR segments of human *FADD* mRNA (GenBank Accession No. NM_003824) and *human caspase-3* mRNA (GenBank accession No. NM_004346) containing the putative miR-155 binding sequence were inserted into the *Eco*RI and *Hin*dIII sites of pGL3-control (Promega, Madison, WI, USA), downstream of the stop codon of the firefly luciferase reporter gene, respectively. HEK 293 cells were co-transfected with 0.8 μg firefly luciferase reporter vector containing the target site, 100 nM miR-155 double-stranded mimics or miR-control (Ambion, Austin, TX, USA) and 0.04 μg *Renilla* luciferase control vector (pRL-TK-Promega), using Lipofectamine 2000 (Invitrogen). Assays were performed 48 h after transfection, using the dual luciferase reporter assay system (Promega). Firefly luciferase activity was normalized to *Renilla* luciferase activity.

The mutation on miR-155 binding sites in human FADD and caspase-3 3′-UTRs were generated using the Quick Change XL Site-Directed Mutagenesis kit (Stratagene, La Jolla, CA, USA)(see Supporting information, Table S1). Each mutation consisted of replacing four consecutive base pairs at the 3′ region of the site.

In vitro up-regulation and knockdown of miR-155

NP cell culture

NP cells were isolated by enzymatic digestion for 40 min at 37 °C in PBS with 0.25% pronase (Gibco-BRL, Carlsbad, CA, USA). The pronase containing solution was removed, remaining tissue washed, and digested for 4 h in PBS with 0.025% collagenase type II (Invitrogen). The digest was filtered through a 45 μm pore size nylon mesh. Cells were plated and expanded for 3 weeks in DMEM/F12-based culture medium, containing 15% fetal bovine serum (FBS; Gibco-BRL) and 1% penicillin/streptomycin (Invitrogen) in a 5% CO_2 incubator. The culture medium was changed twice a week. Primarily cultured NP cells (passage 1) were used for *in vitro* modulation of miR-155.

Up-regulation of miR-155

The lentiviral vector labelled with green fluorescent protein (GFP) encoding pre-miR-155 and a scrambled sequence for control were purchased from Invitrogen. Human NP cells were plated at a density of 1.5×10^5 cells/well in a 24-well plate in a final volume of 250 μl complete medium. Viral solutions at a multiplicity of infection (MOI) of 10 were added to NP cells. Following 5 h of incubation at 37 °C, the cells were allowed to recover over the ensuing 96 h in culture medium. To verify cell transfection, culture flasks were detected by fluorescent microscopy. Subsequently, cells were treated with or without recombinant human FasL (100 ng/ml; R&D, Minneapolis, MO, USA) for 24 h and evaluated by western blot, using standard protocols. In brief, proteins were extracted using RIPA lysis buffer and electrophoresed on Nu-Page gels (Invitrogen), using 100 μg protein/sample. The proteins were transferred to a polyvinylidene difluoride membrane (Invitrogen) and blocked in PBS containing 5% fat-free milk powder. Subsequently, antibodies against FADD (Abcam) and caspase-3 (Abcam) were used to detect the proteins. Goat anti-rabbit immunoglobulin conjugated to horseradish peroxidase (Sigma, St. Louis, MO, USA) was used as the secondary antibody. The immunoreactive proteins were detected using Pierce ECL western blotting substrate (Pierce Biotechnology, Rockford, CA, USA).

Knockdown of miR-155

The lentiviral vector labelled with GFP encoding antigomiR-155 and lentiviral vector control were purchased from Invitrogen. The knockdown of miR-155 in cultured NP cells was achieved by transfection with lentiviral antigomiR-155 with a MOI of 10, as aforementioned. FADD and caspase-3 activities were analysed by western blot as aforementioned.

Apoptosis assay: flow cytometry (FCM)

To identify apoptosis in NP cells, we performed FCM with APC Annexin V/7-AAD (BD Biosciences, San

Diego, CA, USA) staining upon the aforementioned treated NP cells, ie NP cells treated with or without FasL, NP cells transfected with pre-miR-155 or control and treated with FasL, NP cells transfected with antigomiR-155 or control and treated with FasL. In brief, after washing twice with PBS, 1×10^6 cells were resuspended in binding buffer. APC Annexin V and 7-AAD were added and then incubated at room temperature for 15 min. The samples were analysed by FCM.

Transmission electron microscopy

Specimens of NP were fixed in a mixture of 2% paraformaldehyde and 2% glutaraldehyde with phosphate buffer, pH 7.4, and postfixed in a 1% solution of osmium tetroxide with 1.5% potassium ferrocyanide. After being dehydrated in graded alcohols, the samples were embedded in Epon. Ultra-thin sections were prepared and contrasted with uranyl acetate and lead citrate. The sections were studied using a transmission electron microscope (JEM 2000 EX, Japan Electron Organization, Tokyo, Japan) with an accelerating voltage of 80 kV.

Statistical analysis

Comparisons of two-group parameters were performed using Student's t-test. Comparisons of multiple group data were performed using one-way analysis of variance followed by Turkey's post-test. Differences with $p < 0.05$ were considered statistically significant. The statistical analysis was performed using the SPSS statistical package (SPSS, Chicago, IL, USA).

Results

miRNAs are differentially expressed and miR-155 is down-regulated in degenerative NP

In a preliminary study, a routine RNA extraction protocol was performed to prepare total RNAs and a poor amount or quality of RNA was generated, which suggested that the dense ECM precluded the proper preparation of RNAs from sparse NP cells. In order to remove ECM while maintaining the original status of miRNAs, we pre-digested NP tissues with pronase and collagenase (Figure 1A), which significantly improved the efficiency of subsequent RNA extraction from fresh isolated NP cells rather than cultured cells. The microarray data were submitted to the GEO database under the Accession No. GSE19943, following the MIAME guidelines.

Amongst the 678 human miRNAs analysed, 29 miRNAs exhibited significantly differential expression in degenerative NP cells (Figure 1B). The heat map (Figure 1C) indicates the result of a two-way hierarchical clustering of miRNAs and samples. miR-155 was down-regulated 0.41-fold with statistical significance ($p < 0.05$) in degenerative NP, which was further confirmed by semi-quantitative RT–PCR (0.56 ± 0.17-fold, $n = 6$; Figure 1D). Given the unique hallmarks of miR-155 and its roles in immunological responses and apoptotic pathways, we selected miR-155 for subsequent profound investigation to shed light on the aetiology of IDD.

miR-155 inhibits FADD and caspase-3 expression and regulates Fas-mediated apoptosis by directly targeting their 3′-UTRs in human NP cells

Computational analysis and online available miRBase Target Database have facilitated miRNAs target prediction and further prediction validation. We searched the target sites using a miRNAs target prediction software, known as miRTarG (http://mirtar.mbc.nctu.edu.tw), which indicated that the hsa-miR-155 target sites might be harboured in the 3′-UTR of *hFADD* mRNA as well as in the 3′-UTR of *hCASP3* mRNA. Moreover, RNA hybrid analysis [37] provided further evidence demonstrating the potential binding duplexes of the 3′-UTRs of FADD and caspase-3 with miR-155 (Figure 2A). As validation of the computational prediction, the relative luciferase activity was distinctly diminished ($p < 0.05$) in cells co-transfected with miR-155 double-stranded mimics (Figure 2B). Moreover, mutation with four consecutive base pairs of the miR-155 binding sites of FADD and caspase-3 evidently abrogated the repression of luciferase activity due to miR-155 over-expression (Figure 2A, B). These results indicate that miR-155 can inhibit gene expression by targeting the 3′-UTRs of the *hFADD* and *hCASP3* mRNAs.

Western blotting

The GFP expressing lentiviral vector at a MOI of 10 that contains pre-miR-155 or antigomiR-155 resulted in high-level GFP expression in NP cells (Figure 3A). FasL treatment in NP cells caused concurrent up-regulation of both FADD and caspase-3. Up-regulation of miR-155 with pre-miR-155 resulted in repression of FADD and caspase-3, whereas knockdown of miR-155 with antigomiR-155 led to over-expression of FADD and caspase-3 in NP cells. In contrast, lentiviral vector control with scramble sequences produced no significant effects on the expression of FADD and caspase-3 (Figure 2C).

FCM assay

Given that NP cells transfected with lentivirus expressing GFP spectrally overlap between FITC–annexin V and GFP, APC annexin-V in conjunction with 7-AAD was used to avoid the overlap. As expected, approximately $6.7 \pm 0.93\%$ of untreated cultured NP cells were apoptotic. FasL treatment in NP cells resulted in significant increase in apoptotic cells ($23.8 \pm 1.22\%$; $p < 0.05$). Furthermore, the apoptotic cells were decreased significantly when using pre-miR-155 to over-express miR-155 in NP cells and followed with

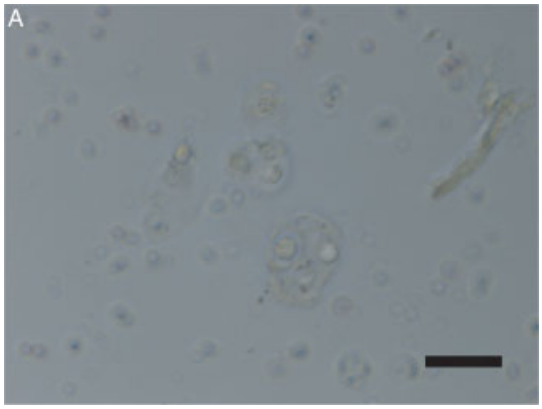

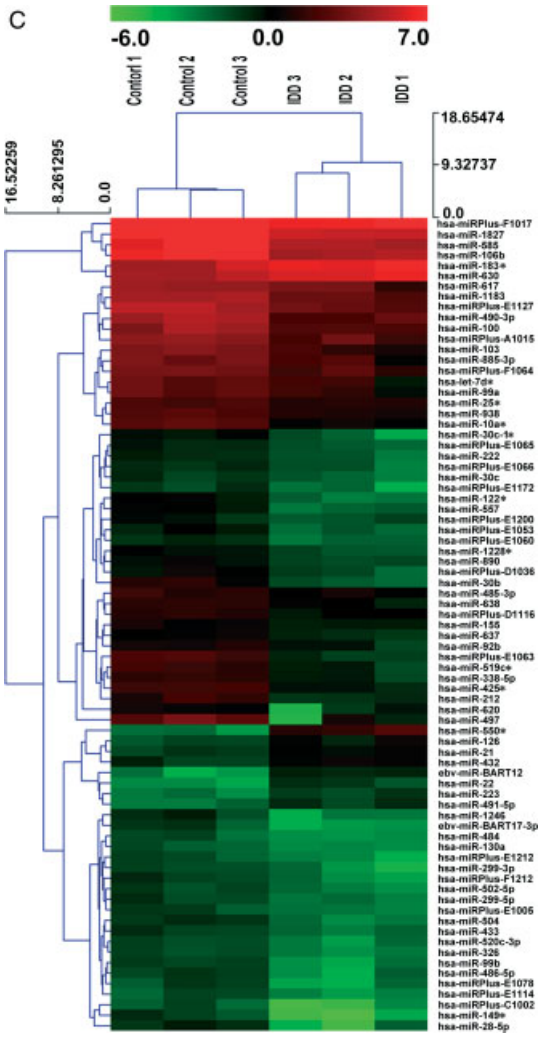

B miRNAs	Fold change	*P*
Up regulated miRNAs		
miR-27a	2.646	1.847 E-02
miR-450b-3	3.018	2.161 E-02
miR-551b	2.318	2.787 E-02
miR-640	23.864	2.351 E-02
miR-1286	6.066	2.898 E-02
miR-1288	2.731	1.160 E-02
Down regulated miRNAs		
miR-129-5p	0.328	2.682 E-02
miR-155	0.410	4.477 E-02
miR-198	0.386	4.433 E-02
miR-382	0.384	1.279 E-03
miR-483-5p	0.270	3.344 E-04
miR-490-5p	0.433	1.251 E-02
miR-492	0.287	3.315 E-02
miR-508-5p	0.363	4.900 E-02
miR-510	0.340	1.605 E-02
miR-552	0.372	1.248 E-02
miR-595	0.301	1.976 E-02
miR-623	0.410	5.429 E-03
miR-625	0.374	1.237 E-02
miR-638	0.224	2.518 E-03
miR-663	0.186	1.014 E-02
miR-671-5p	0.393	2.030 E-02
miR-744	0.458	3.667 E-02
miR-886-3p	0.336	2.192 E-02
miR-886-5p	0.343	1.237 E-02
miR-874	0.305	3.703 E-02
miR-1249	0.324	4.109 E-02
miR-1258	0.489	1.962 E-02
miR-1275	0.211	9.248 E-04

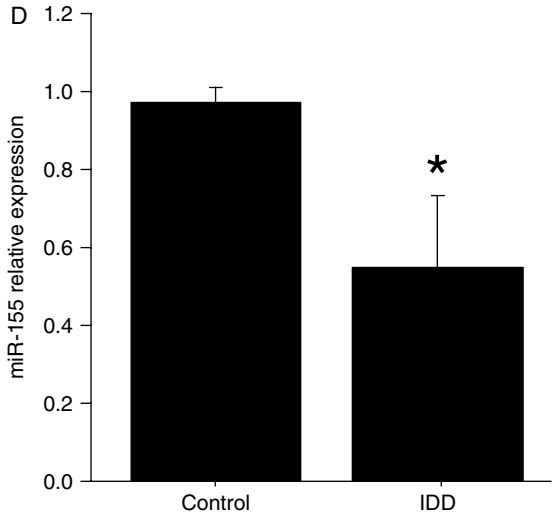

Figure 1. miRNAs are differentially expressed and miR-155 is down-regulated in human degenerative NP compared with control NP. (A) Representative photomicrograph of human digested NP. Note that NP cells keep their round morphology with cell clusters. Scale bar = 200 μm. (B) Summary of 29 significantly differentially expressed miRNAs. (C) The heat map shows the result of the two-way hierarchical clustering of miRNAs and samples. Amongst the differentially expressed miRNAs, miR-155 was selected for subsequent profound investigation, due to its unique hallmarks and roles in immunological responses and apoptotic pathways. (D) miR-155 is down-regulated in degenerative NP. Data are representative of six independent experiments. Error bars represent SEM. $^{*}p < 0.05$.

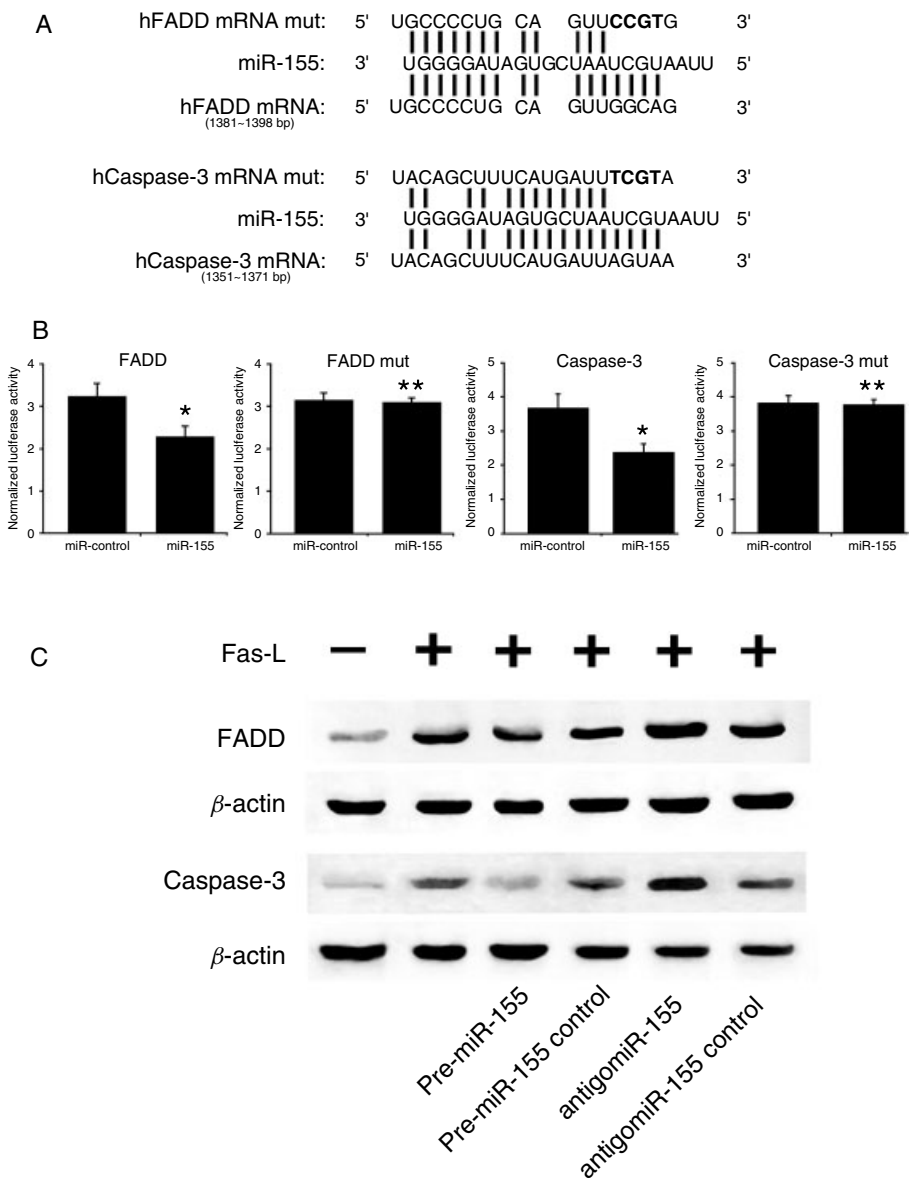

Figure 2. miR-155 can inhibit FADD and caspase-3 via targeting the 3′-UTRs of FADD and caspase-3. (A) Complementarity between miR-155 and the putative hFADD 3′-UTR target site (above) as well as the hCaspase-3 3′-UTR target site (below). hFADD-mut and hCaspase-3-mut indicate the FADD and caspase-3 3′-UTRs with four consecutive mutation sites (in bold) in miR-155 binding sites. (B) The relative luciferase activities of three independent experiments are shown. Error bars represent SEM. $^{*}p < 0.05$; $^{**}p > 0.05$. (C) Western blot analysis of total FADD and caspase-3 protein levels of human NP cells with up-regulation and knockdown of miR-155.

FasL treatment ($12.1 \pm 1.43\%$; $p < 0.05$); whereas the apoptotic cells were increased when antagonizing miR-155 in NP cells and followed with FasL treatment ($31.3 \pm 2.21\%$; $p < 0.05$) (Figure 3B, C). In contrast, the impact of lentiviral vector control with scramble sequences of pre-miR-155 or antigomiR-155 on apoptosis was insignificant ($24.7 \pm 2.1\%$; $25.0 \pm 2.6\%$). Together, these results indicated that Fas-mediated apoptosis was increased when antagonizing miR-155 and decreased when using pre-miR-155 in human NP cells.

Apoptosis increases and cell clusters in IDD samples

As shown in Figure 4, apoptotic NP cells from control samples were rare, but apoptotic NP cells from IDD samples were relatively abundant. Furthermore, apoptotic cells in both early phase and late phase with apoptotic bodies were noted. As degenerative hallmarks of IDD, cell clusters with variety in morphology and size were noted (Figure 5).

miR-155 expression in the cytoplasm of human NP cells is reversely correlated with FADD and caspase-3

As shown in Figure 6, miR-155 was expressed by human NP cells, whether degenerative or not. Furthermore, miR-155 localized in the cytoplasm of human NP cells of both IDD and control samples. However, ISH with scramble LNA probes resulted in no blue signals within NP cells as negative controls. On the other hand, as the putative targets of miR-155 in IDD,

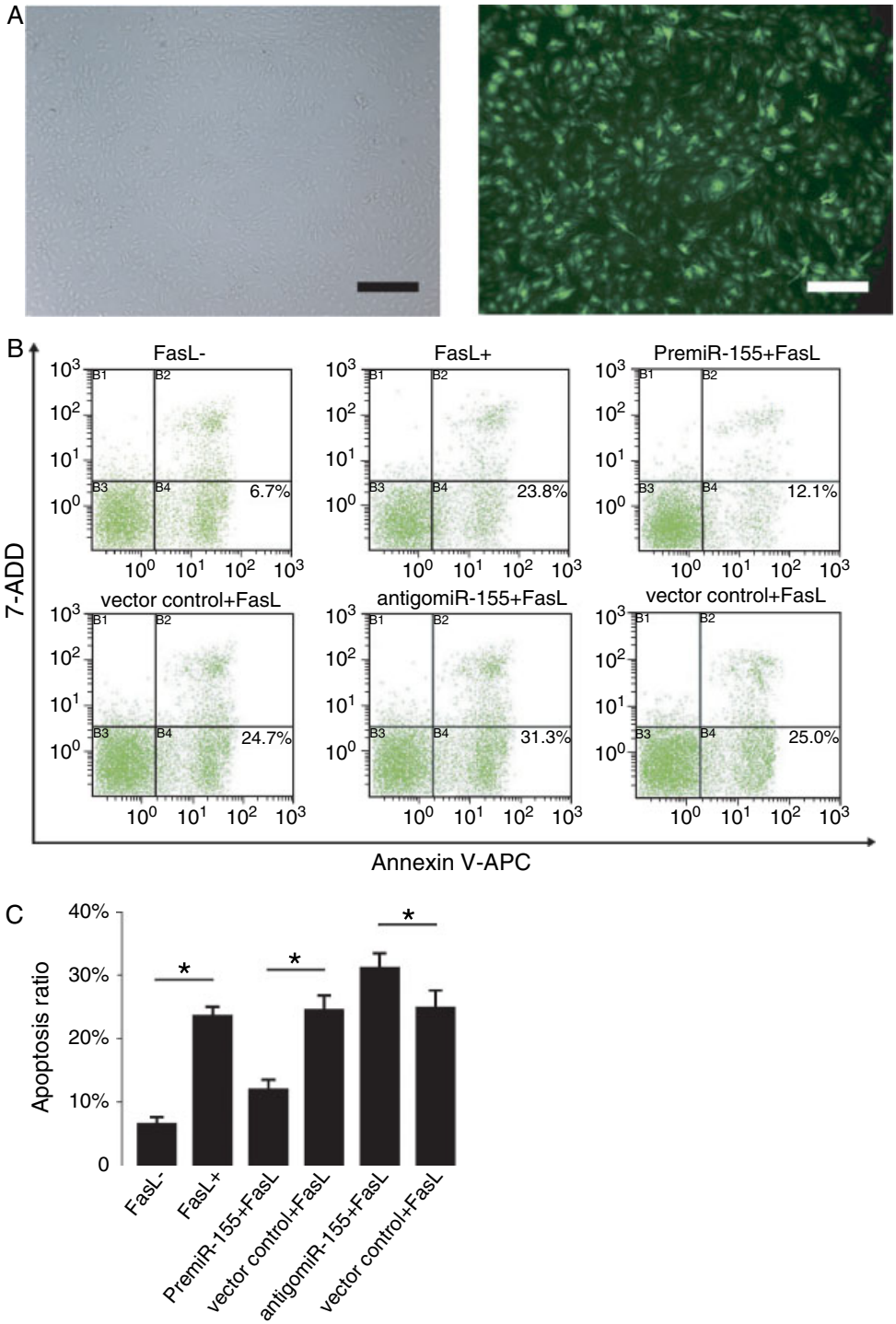

Figure 3. Fas-mediated apoptosis was increased when antagonizing miR-155 and decreased when using pre-miR-155 in human NP cells. (A) Brightfield (left) and fluorescent (right) microscopy of human NP cells 96 h following transfection with lentivirus labelled with GFP. Scale bars = 500 μm. (B) Contour diagram of APC-annexin V/7-AAD FCM of human NP cells. The graphs represent typical results of cell apoptosis; values represent the means for three experiments. (C) Comparison of apoptotic cells in various NP cells groups ($^*p < 0.05$). Data are representative of three experiments; error bars represent SEM.

FADD and caspase-3 were detected in the cytoplasm of human NP cells under both brightfield (DAB reaction with brown) and dark-field (Figure 7) illumination. miR-155, FADD and caspase-3 were noted in NP cell clusters with multiple nuclei or in single NP cells.

To further identify the spatial distribution of miR-155 and its targets, we used ISH and IHC double labelling in the same section, with ISH histochemistry as previously described [35, 36]. Double labelling showed that miR-155-positive NP cells were FADD- and caspase-3-negative, and the FADD- and caspase-3-positive NP cells were miR-155-negative. Together, these results confirmed that miR-155 expressed in human NP and miR-155 down-regulated FADD and caspase-3.

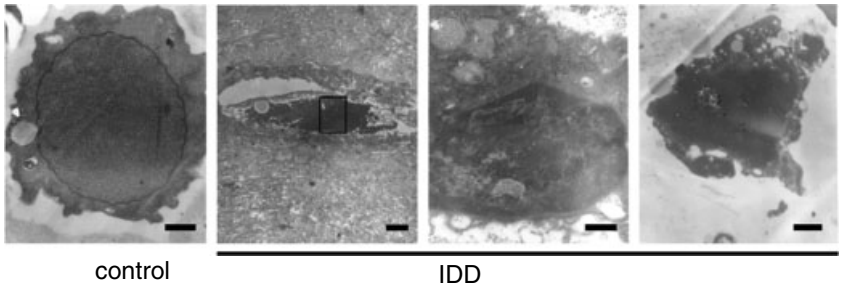

Figure 4. NP cells apoptosis increases in IDD samples compared to control samples. Typical viable NP cell from control samples and apoptotic NP cells from IDD samples are shown. The area surrounded by the black box is enlarged in the right panel. Scale bars = 0.4, 1, 0.2 and 0.5 μm (from left to right).

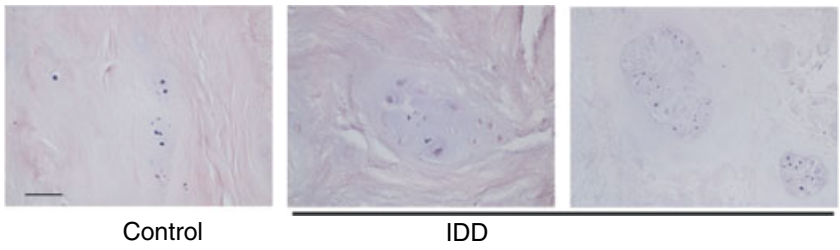

Figure 5. H&E staining of control and degenerative intervertebral discs. Cell clusters in various sizes. Scale bar = 50 μm.

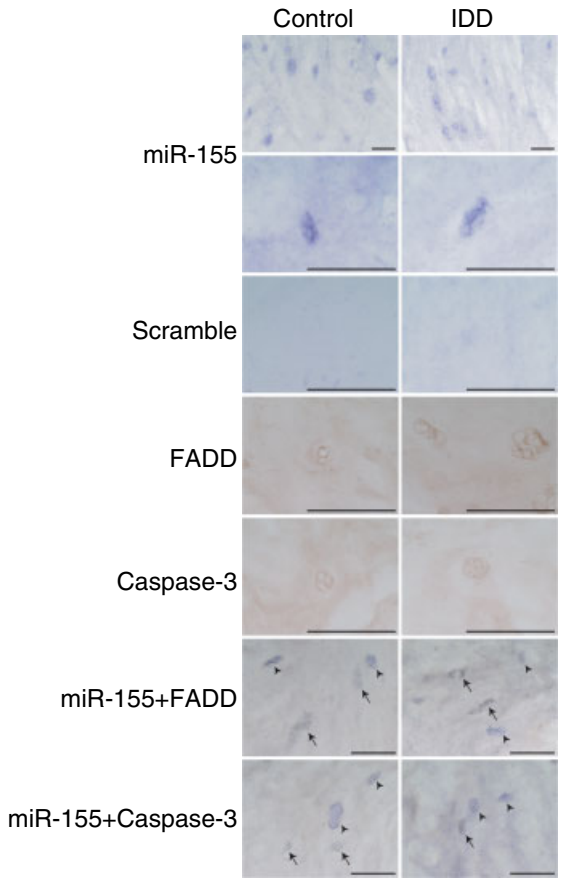

Figure 6. Expression of miR-155 (blue) is confined to the cytoplasm of human control and degenerative NP cells with attendant reverse expression of FADD and caspase-3. FADD and caspase-3 expression (brown) localizes in the cytoplasm near the membrane of NP cells. miR-155-positive NP cells (arrowheads) were FADD- and caspase-3-negative, and FADD- and caspase-3-positive NP cells (arrows) were miR-155-negative. Scale bars = 200 μm.

Discussion

Here we provide evidence for a mechanistic link between increased Fas-mediated apoptosis and decreased miR-155 in IDD. We explored miRNAs, in particular miR-155, as regulators in human IDD and found that: (a) miRNAs are differentially expressed and miR-155 is down-regulated in human degenerative NP; (b) miR-155 can inhibit FADD and caspase-3 by directly targeting the 3′-UTRs of FADD and caspase-3: *in vitro* miR-155 repression results in the up-regulation of FADD and caspase-3 and consequently increased apoptosis of NP cells; (c) miR-155 localizes in the cytoplasm of human NP cells with a reverse expression pattern to FADD and caspase-3. These results revealed that the deregulated miR-155 might play a role in the pathogenesis of IDD by increasing Fas-mediated apoptosis. Moreover, miR-155 might be a potentially novel therapeutic target for IDD using the lentiviral-mediated pre-miR-155.

While the role of other differentially expressed miRNAs identified in our study remains to be investigated, the function, expression and targets of miR-155 are relatively clear. The direct targets of miR-155 can be categorized into transcriptional regulatory genes, protein receptors, kinases, nuclear proteins and binding proteins within specific cells [38]. Although miR-155 was first confirmed to target FADD by Tili and colleagues in mice [28], our *in vitro* modulation of miR-155 in cultured human NP cells provides beneficial points of clinical relevance. On the other hand, Ovcharenko *et al* [39] reported that up-regulation of miR-155 decreases TNF-related apoptosis-inducing ligand (TRAIL)-induced caspase-3 activity in the breast cancer cell line, MDA-MB-453, via a yet-undefined mechanism. Our reporter gene and *in vitro*

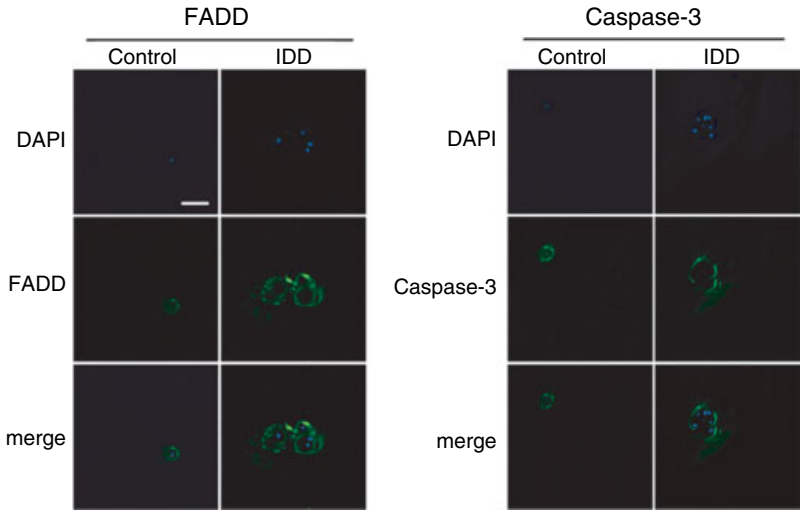

Figure 7. Expression of FADD and caspase-3 is detected by fluorescent probes in dark field. FADD and caspase-3 expression is present in the cytoplasm near the membrane within a single NP cell in control or cell clusters with multiple nuclei in degenerative NP. Scale bar = 40 μm.

modulation of miR-155 on caspase-3 expression verified the prediction that miR-155 directly targets caspase-3 in the FasL-induced apoptotic pathway.

Recent LNA probes-based LNA–ISH has made it possible to spatially localize miRNAs at tissue, cellular and even subcellular levels in tissue sections [33,35]. Furthermore, a combination of ISH and IHC provides novel evidence demonstrating the colocalization of a single miRNA and its putative target. However, literature addressing the spatial localization of miR-155 in human tissues is sparse. This might be partly due to the relatively low copy number of miR-155 in human tissues, according to Liang *et al* [40]. The maximum copy number of miR-155 (as low as 476) is reported in human lymph node, which might add difficulties to LNA–ISH. Martin *et al* [41] noted that miR-155 localized in the cytoplasm in the smooth muscle layer and epithelium of human lung as well as in the endothelium of human placenta. Nuovo *et al* [35] identified miR-155 in a number of human tissues with lymphoproliferative diseases and cancer, where miR-155 localized in cytoplasm with or without colocalization of putative targets. We not only localized miR-155 and its targets in human NP, but also double-labelled miR-155 and its two targets, which provides direct supporting evidence to a direct role for miR-155 in FADD and caspase-3 regulation.

While we suggest that deregulated miR-155 promotes Fas-dependent apoptosis in NP cells, the derivation of FasL is noteworthy. Virtually, there are several lines of evidence suggesting that FasL might be derived from local NP cells and invading CTLs. First, both FasL and Fas are expressed by human T lymphocytes [42] and human NP cells [16,17,43]. Second, the FasL–Fas network is involved in the apoptotic pathways and immune privilege [44]. Therefore, the immune privilege as well as the apoptosis of human NP might depend on the interaction of human NP cells and invading CTLs via the FasL–Fas network. However, the important issue of FasL derivation and immune privilege alterations upon IDD need to be well defined.

There are several limitations to our present study. For example, scoliosis discs were used as control discs, although such materials are not fully normal histologically [45]. However, we exploited the universal scheme for these patients, ie the grading scheme for disc degeneration [30] to minimize between-group variations other than degeneration. Nevertheless, it should be noted that miRNAs are, on average, 22 nucleotide small RNAs with the features of instability and susceptibility to degradadation. Therefore, it is the restriction of miRNAs that excludes the possibility of using cadaveric discs. Another potential limitation of the study is the relatively restricted samples for microarray analysis. However, miRNAs microarray is a preliminary screening which has been further validated using RT–PCR with sufficient samples. We extracted miRNAs from freshly isolated NP cells, although we tried the traditional RNA extraction procedure from human NP tissues. The low amount of RNA obtained from NP tissues might be due to the inherently low NP cellularity in human discs, with NP cells making up only approximately 1% of the total volume [46]. In addition, the predigestion procedure without culture excludes ECM while maintaining the original round shape of NP cells (Figure 1A), and consequently might minimize the loss of miRNAs. From this point of view, it might be helpful to study miRNAs in similar musculoskeletal tissues, such as cartilage.

In conclusion, we find that caspase-3 is a novel target of miR-155 and that deregulated miR-155 promotes Fas-mediated apoptosis in human IDD by targeting FADD and caspase-3, implicating a role of miR-155 in the aetiology of IDD. Moreover, miR-155 might potentially be a therapeutic target for IDD by using the lentiviral pre-miR-155.

Acknowledgment

This study was supported by the Chinese National Natural Science Foundation (Grant Nos 30901509, 30770571 and 30973052), the Key Technologies R&D Programme of Shaanxi Province (Grant No. 2008K10-02) and the Chinese National Basic Research Program (Grant No. 2009CB521700). We thank Dr Yan-Yan Wei for her assistance in ISH and IHC staining; our clinical staff for helping obtain specimens; our office secretary Dan Geng for her coordination of the experimentation; laboratory members Li-Feng Lan, Jie Wu and Jing Li for their assistance in the experimentation; and Kang Chen Bio-tech (Shanghai, China) for their skillful assistance on microRNA microarray.

Author contributions

HQW, XC and ZJL conceived the study; HQW, XDY, ZHL, XC, SXW, JH and CJ carried out experiments; and HQW, DS, LTJ and ZJL analysed data. All authors were involved in writing the paper and had final approval of the submitted and published versions.

Abbreviations

FADD, Fas-associated death domain-containing protein; FCM, flow cytometry; IDD, intervertebral disc degeneration; IHC, immunohistochemistry; ISH, *in situ* hybridization; LNA, locked nucleic acid; NP, nucleus pulposus; TEM, transmission electron microscopy; 3′-UTR, 3′-untranslated region.

References

1. Waddell G. Low back pain: a twentieth century health care enigma. *Spine* 1996; **21**: 2820–2825.
2. Anderson GB. Epidemiological features of chronic low-back pain. *Lancet* 1999; **354**: 581–585.
3. Aladin DMK, Cheung KMC, Chan D, *et al*. Expression of the *Trp2* allele of *COL9A2* is associated with alterations in the mechanical properties of human intervertebral discs. *Spine* 2007; **32**: 2820–2826.
4. Solovieva S, Lohiniva J, Leino-Arjas P, *et al*. Intervertebral disc degeneration in relation to the COL9A3 and the IL-1β gene polymorphisms. *Eur Spine J* 2006; **15**: 613–619.
5. Tschoeke SK, Hellmuth M, Hostmann A, *et al*. Apoptosis of human intervertebral discs after trauma compares to degenerated discs involving both receptor-mediated and mitochondrial-dependent pathways. *J Orthop Res* 2008; **26**: 999–1006.
6. Jones P, Gardner L, Menage J, *et al*. Intervertebral disc cells as competent phagocytes *in vitro*: implications for cell death in disc degeneration. *Arthritis Res Ther* 2008; **10**: R86.
7. Stokes IA, Iatridis JC. Mechanical conditions that accelerate intervertebral disc degeneration: overload versus immobilization. *Spine* 2004; **29**: 2724–2732.
8. Guehring T, Omlor GW, Lorenz H, *et al*. Stimulation of gene expression and loss of annular architecture caused by experimental disc degeneration—an *in vivo* animal study. *Spine* 2005; **30**: 2510–2515.
9. Murata Y, Olmarker K, Larsson K, *et al*. Production of tumor necrosis factor-α from porcine nucleus pulposus cells at various time points in cell culture under conditions of nutritional deficiency. *Cytokine* 2006; **34**: 206–211.
10. Zeng Y, Danielson KG, Albert TJ, *et al*. HIF-1α is a regulator of galectin-3 expression in the intervertebral disc. *J Bone Miner Res* 2007; **22**: 1851–1861.
11. Rutges JPHJ, Kummer JA, Oner FC, *et al*. Increased MMP-2 activity during intervertebral disc degeneration is correlated to MMP-14 levels. *J Pathol* 2008; **214**: 523–530.
12. Griffith TS, Brunner T, Fletcher SM, *et al*. Fas ligand-induced apoptosis as a mechanism of immune privilege. *Science* 1995; **270**: 1189–1192.
13. Nagata S, Golstein P. The Fas death factor. *Science* 1995; **267**: 1449–1456.
14. Trout JJ, Buckwalter JA, Moore KC. Ultrastructure of the human intervertebral disc: II. Cells of the nucleus pulposus. *Anat Rec* 1982; **204**: 307–314.
15. Hunter CJ, Matyas JR, Duncan NA. The notochordal cell in the nucleus pulposus: a review in the context of tissue engineering. *Tissue Eng* 2003; **9**: 667–677.
16. Takada T, Nishida K, Doita M, *et al*. Fas ligand exists on intervertebral disc cells: a potential molecular mechanism for immune privilege of the disc. *Spine* 2002; **27**: 1526–1530.
17. Park J-B, Kim K-W, Han C-W, *et al*. Expression of Fas receptor on disc cells in herniated lumbar disc tissue. *Spine* 2001; **26**: 142–146.
18. Nagata S. Apoptosis by death factor. *Cell* 1997; **88**: 355–365.
19. Hitomi J, Christofferson DE, Ng A, *et al*. Identification of a molecular signaling network that regulates a cellular necrotic cell death pathway. *Cell* 2008; **135**: 1311–1323.
20. Krammer PH. CD95's deadly mission in the immune system. *Nature* 2000; **407**: 789–795.
21. Jovanovic M, Hengartner MO. miRNAs and apoptosis: RNAs to die for. *Oncogene* 2006; **25**: 6176–6187.
22. Bartel DP. MicroRNAs: genomics, biogenesis, mechanism, and function. *Cell* 2004; **116**: 281–297.
23. Sonkoly E, Stahle M, Pivarcsi A. MicroRNAs and immunity: novel players in the regulation of normal immune function and inflammation. *Semin Cancer Biol* 2008; **18**: 131–140.
24. Selbach M, Schwanhausser B, Thierfelder N, *et al*. Widespread changes in protein synthesis induced by microRNAs. *Nature* 2008; **455**: 58–63.
25. Worm J, Stenvang J, Petri A, *et al*. Silencing of microRNA-155 in mice during acute inflammatory response leads to derepression of c/ebpβ and down-regulation of G-CSF. *Nucleic Acids Res* 2009; **37**: 5784–5792.
26. Teng G, Papavasiliou FN. Shhh! Silencing by microRNA-155. *Phil Trans R Soc Lond B Biol Sci* 2009; **364**: 631–637.
27. Park SM, Peter ME. microRNAs and death receptors. *Cytokine Growth Factor Rev* 2008; **19**: 303–311.
28. Tili E, Michaille JJ, Cimino A, *et al*. Modulation of miR-155 and miR-125b levels following lipopolysaccharide/TNFα stimulation and their possible roles in regulating the response to endotoxin shock. *J Immunol* 2007; **179**: 5082–5089.
29. Dorsett Y, McBride KM, Jankovic M, *et al*. MicroRNA-155 suppresses activation-induced cytidine deaminase-mediated Myc-Igh translocation. *Immunity* 2008; **28**: 630–638.
30. Pfirrmann CWA, Metzdorf A, Zanetti M, *et al*. Magnetic resonance classification of lumbar intervertebral disc degeneration. *Spine* 2001; **26**: 1873–1878.
31. Liu CG, Calin GA, Meloon B, *et al*. An oligonucleotide microchip for genome-wide microRNA profiling in human and mouse tissues. *Proc Natl Acad Sci USA* 2004; **101**: 9740–9744.

32. Livak KJ, Schmittgen TD. Analysis of relative gene expression data using real-time quantitative PCR and the $2^{-\Delta\Delta Ct}$ method. *Methods* 2001; **25**: 402–408.
33. Obernosterer G, Martinez J, Alenius M. Locked nucleic acid-based *in situ* detection of microRNAs in mouse tissue sections. *Nat Protoc* 2007; **2**: 1508–1514.
34. Silahtaroglu AN, Nolting D, Dyrskjot L, *et al*. Detection of microRNAs in frozen tissue sections by fluorescence *in situ* hybridization using locked nucleic acid probes and tyramide signal amplification. *Nat Protoc* 2007; **2**: 2520–2528.
35. Nuovo GJ, Elton TS, Nana-Sinkam P, *et al*. A methodology for the combined *in situ* analyses of the precursor and mature forms of microRNAs and correlation with their putative targets. *Nat Protoc* 2009; **4**: 107–115.
36. Huang J, Feng F, Tamamaki N, *et al*. Prenatal and postnatal development of GABAergic neurons in the spinal cord revealed by green fluorescence protein expression in the GAD67-GFP knock-in mouse. *Neuroembryol Aging* 2007; **4**: 147–154.
37. Rehmsmeier M, Steffen P, Hochsmann M, *et al*. Fast and effective prediction of microRNA/target duplexes. *RNA* 2004; **10**: 1507–1517.
38. Faraoni I, Antonetti FR, Cardone J, *et al*. *miR-155* gene: a typical multifunctional microRNA. *Biochim Biophys Acta* 2009; **1792**: 497–505.
39. Ovcharenko D, Kelnar K, Johnson C, *et al*. Genome-scale microRNA and small interfering RNA screens identify small RNA modulators of TRAIL-induced apoptosis pathway. *Cancer Res* 2007; **67**: 10782–10788.
40. Liang Y, Ridzon D, Wong L, *et al*. Characterization of microRNA expression profiles in normal human tissues. *BMC Genom* 2007; **8**: 166.
41. Martin MM, Buckenberger JA, Jiang J, *et al*. The human angiotensin II type 1 receptor +1166 A/C polymorphism attenuates microrna-155 binding. *J Biol Chem* 2007; **282**: 24262–24269.
42. Chervonsky AV, Wang Y, Wong FS, *et al*. The role of Fas in autoimmune diabetes. *Cell* 1997; **89**: 17–24.
43. Park J-B, Chang H, Kim K-W. Expression of Fas ligand and apoptosis of disc cells in herniated lumbar disc tissue. *Spine* 2001; **26**: 618–621.
44. Lee H-O, Ferguson TA. Biology of FasL. *Cytokine Growth Factor Rev* 2003; **14**: 325–335.
45. Roberts S, Menage J, Eisenstein SM. The cartilage end-plate and intervertebral disc in scoliosis: calcification and other sequelae. *J Orthop Res* 1993; **11**: 747–757.
46. Roberts S, Evans H, Trivedi J, *et al*. Histology and pathology of the human intervertebral disc. *J Bone Joint Surgery Am* 2006; **88**: 10–14.

SUPPORTING INFORMATION ON THE INTERNET

The following supporting information may be found in the online version of this article:

Table S1. Primers used in RT–PCR and mutation.

Table S2. Microarray summary of GSE19943.

Supporting Data File. Supporting file. Fold changes and *P*-values of GSE19943.